Nonlinear Effects of Three-phase Diode Rectifier on Noise Emission in the Frequency Range of 2–9 kHz

Rathnayake, Hansika; Zare, Firuz; Kumar, Dinesh; Ganjavi, Amir; Davari, Pooya

Published in:
2020 IEEE International Conference on Power Electronics, Drives, and Energy Systems (PEDES 2020)

DOI (link to publication from Publisher):
10.1109/PEDES49360.2020.9379749

Publication date:
2020

Document Version
Accepted author manuscript, peer reviewed version

Nonlinear Effects of Three-phase Diode Rectifier on Noise Emission in the Frequency Range of 2-9 kHz

Hansika Rathnayake
School of Information Technology and Electrical Engineering
The University of Queensland
Brisbane Qld 4072, Australia
h.rathnayake@uq.edu.au

Firuz Zare
School of Information Technology and Electrical Engineering
The University of Queensland
Brisbane Qld 4072, Australia
f.zare@uq.edu.au

Dinesh Kumar
Global Research and Development Center
Danfoss Drives A/S
6300 Gråsten, Denmark
dineshr30@ieee.org

Amir Ganjavi
School of Information Technology and Electrical Engineering
The University of Queensland
Brisbane Qld 4072, Australia
a.ganjavi@uq.net.au

Pooya Davari
Dept. of Energy Technology
Aalborg University
Aalborg, Denmark
pda@et.aau.dk

***Abstract*— This paper presents a study on differential mode noise emission affected by a three-phase diode rectifier when there is an input Electromagnetic Interference (EMI) filter. The EMI filter is generally designed for noise attenuation beyond 150 kHz. Therefore, systematic analysis of its behaviour in the new frequency range of 2-9 kHz is essential to identify its unacceptable noise emissions. This is important to comply with upcoming emission standards in the frequency range of 2-9 kHz. This paper presents the impact of a three-phase diode rectifier and an EMI filter in different system damping conditions, different grid types and switching frequencies regarding the harmonic emission in the frequency range of 2-9 kHz. The accuracy of a proposed equivalent circuit model of EMI filter to predict grid current emissions is also evaluated for above system conditions, leading to recommendations to noise reduction at 2-9 kHz.**

***Keywords*— Differential mode noise, 2-9 kHz emission, three-phase motor drive, EMI filter, diode-bridge rectifiers**

I. INTRODUCTION

The increased switching frequency of the motor drive systems introduces harmonic emissions at 2-9 kHz frequency range. This issue has become a new interesting research area to be investigated since these unregulated emissions reduce the reliability and efficiency of the overall distribution network and communication systems [1]-[3].

The standards for 2-150 kHz frequency range have not been completed to cover all products including adjustable motor drives, so that IEC Technical Committee 77A is currently working on this new standardisation process [2]. According to IEC activity, the frequency range has been split into two main frequency bands as 2-9 kHz and 9-150 kHz. In parallel to the standardisation activity, recent studies on 2-150 kHz frequency range have been presented in [4]-[8] related to emission modelling of different converter topologies. Even though 2-150 kHz range is new for emission studies, the Differential Mode (DM) emission modelling beyond 150 kHz is well discussed for DC-voltage fed three-phase power converters in [9]-[11] , for grid connected- three-phase buck-type PWM rectifier topology in [12] and for grid connected-three-phase diode rectifier-Inverter topology in [13]. The line-current quality improvement of uncontrolled rectifier topology under normal and unbalanced supply voltage conditions are presented in [14, 15] for the low-frequency range. However, the line-current quality improvement of the three-phase, diode rectifier-Inverter topology in motor drive systems at 2-9 kHz under EMI filter connection, which can introduce resonances, is not considered so far in EMI analysis studies. Therefore, it is vitally important to understand resonances/ unacceptable DM emissions in this frequency range using the already existing EMI filter in the three-phase motor drives, which is only designed to attenuate emissions beyond 150 kHz.

This paper presents a systematic study to demonstrate the impact of input EMI filter to the DM noise at 2-9 kHz frequency range, in a three-phase motor drive system with a nonlinear diode-bridge rectifier at the grid-side. Further, equivalent circuit modelling for the EMI filter is also presented, where the equivalent model accuracy is evaluated compared to the three-phase full system in different system damping conditions. Further, the paper presents the impact of grid type and switching frequency to DM noise level, where the proposed model accuracy is also discussed. Finally, the recommendation for 2-9 kHz noise reduction is discussed using the derived transfer function of the modelled EMI filter. The equivalent circuit modelling for the EMI filter is the key step in the filter modification when the drive manufacturers compete to comply with the upcoming EMI emission standards in 2-9 kHz range. Thus, this paper significantly contributes to accelerating the drive products development and entering the market with possible compliance of upcoming EMI standards for 2-9 kHz frequency range.

II. SYSTEM DESCRIPTION

Three-phase motor drive system with an input EMI filter used for DM analysis simulations is illustrated in Fig. 1(a) with specifications in Table I. The primary noise source for DM emission is generated by the PWM inverter connected to an AC motor at the load side which is indicated as i_{inv}. The frequency spectrum of this noise current at inverter input can be expressed as (1), where $S_{x,inv}$ is the inverter switching function depending on the PWM technique and i_x is motor terminal currents. Further, the total DC link current flowing through DC choke (L_{dc}) is defined as i_{rect}, which depends on the i_{inv} and transfer function of DC-link as expressed in (2). Here, Z_C and Z_L are equivalent DM impedance of DC-link capacitors and inductors, respectively for a conduction instant of a rectifier.

The i_{rect} can be represented as a current source at the rectifier output, as shown in Fig. 1(a). This current source substitutes the system, including DC-link, inverter and motor.

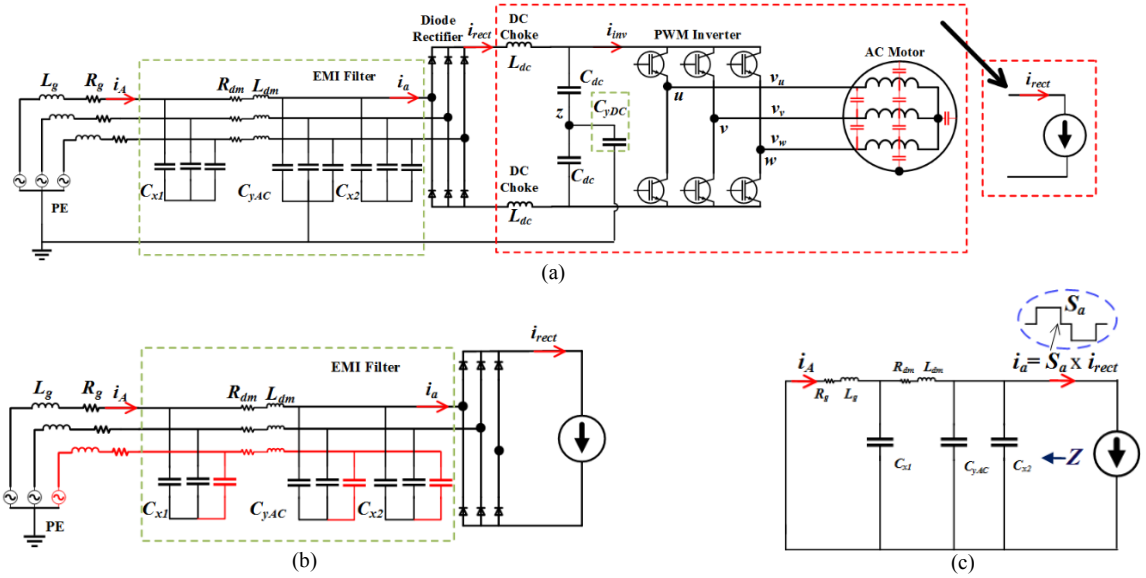

Fig. 1 EMI filter representation in the system (a) The studied three-phase motor drive system with input EMI filter, (b) Simplified general system at each 60° operation of the rectifier, where only two phases conduct through the rectifier (Phase A and B in here), but all three phases can be conducted at the grid side, (c) The proposed equivalent model for analysing the DM noise at the grid

The grid current and rectifier input current of phase A are represented as i_A and i_a, respectively. The leakage inductance introduced by common-mode choke is L_{dm}, in which series resistance is R_{dm}. In this study, an inverter with 5 kHz switching frequency has been mainly considered and i_{inv} signal is related to the switching using Stator Flux-oriented Asynchronous Vector Modulation (SFAVM). The drive-frame connected point of C_{yDC} and C_{yAC} can be disconnected from PE to only analyse the DM noise circulation. Notably, the proposed models in this paper are developed considering continuous conduction mode operation of diode rectifier.

$$i_{inv}(f) = \sum_{x\in\{u,v,w\}} S_{x,inv}(f) \otimes i_x(f) \tag{1}$$

$$i_{rect}(f) = \left(\frac{Z_C}{Z_C + Z_L}\right) i_{inv}(f) \tag{2}$$

TABLE I. SPECIFICATIONS OF THE SELECTED INDUSTRIAL DRIVE SYSTEM

System	Value	EMI filter	Value
L_g, L_{dc}, C_{dc}	0.1 mH, 1.25 mH, 1000 µF	L_{dm}, R_{dm}	21 µH, 0.2 Ω
Switching frequency, Power	5 kHz, 4 kW	C_{x1}, C_{yAC}, C_{x2}, C_{yDC}	1.5 µF, 470 nF, 100 nF, 100 nF

III. INFLUENCE OF DIODE RECTIFIER AND INPUT EMI FILTER ON DM NOISE

In this section, the three-phase full system with and without EMI filter is analysed for DM noise at 2-9 kHz using Matlab/Simulink for a stiff grid. Generally, for a 100 kVA, 415 V distribution system, $L_g = 0.1$ mH explains that the grid is stiff in which the grid impedance is 1.8% of the base impedance for feeders and transformers. In contrast, if the L_g is 1 mH, the grid impedance is 18.2 % of the distribution system's base impedance which makes the grid weak. So, for this section grid is represented by $L_g = 0.1$ mH and $R_g = 0.1$ Ω. The frequency spectrum of i_{inv} consists of a high level of harmonics around 5 kHz as expected (Fig. 2(a)). However, the harmonics beyond 4 kHz including these dominant harmonics have attenuated in the rectifier input current (i_a) due to the DC-link filters, even though harmonics at 2-4 kHz has slightly increased in i_a (Fig. 2(b)). Fig. 2(c) and (d) show the time-domain waveforms for i_A without and with EMI filter, respectively. These results demonstrate that the EMI filter creates new resonances during both 120° conduction mode and commutation mode of rectifier operation. Generally, two phases conduct through diode-rectifier operation in each 60° phase (for example, only phase A, B or B, C or C, A conduct at an instant). Moreover, this non-linearity of the diode rectifier introduces transient effects when a commutation from one phase to another phase happens. These transients create non-periodic, resonances in the EMI filter circuit at the grid side affecting the DM noise level. As in Fig. 2(e), the frequency response comparison of i_A at 2-5 kHz shows there is a harmonic attenuation due to the EMI filter connection. In contrast, there is a clear harmonic amplification of i_A at 5- 9 kHz due to the EMI filter connection. Thus, it is essential to derive an appropriate equivalent circuit model for the system with the EMI filter, which can get rid of the transient effects of the diode rectifier in analysing the DM noise. This modelling is useful to investigate the best possible configuration of the EMI filter to minimise the DM noise at 2-9 kHz.

IV. EQUIVALENT MODEL IMPLEMENTATION FOR INPUT EMI FILTER CONNECTED DIODE-RECTIFIER SYSTEM

The non-linearity of the diode rectifier is created by its switching function $S_{y,rect}$ ($y = a, b, c$), so that the rectifier input current, i_y ($y = a, b, c$) is a function of $S_{y,rect}$ and i_{rect}, which can be expressed as (3).

$$i_y(t) = S_{y,rect}(t) \times i_{rect}(t), \quad y \in \{a, b, c\} \tag{3}$$

When there is no EMI filter, the rectifier directly connects to the grid impedance and there is no resonance effect. Then the equivalent circuit at the grid side can simply be modelled assuming there are only two phases connected in series at the grid side [16]. However, as discussed, when there is an EMI

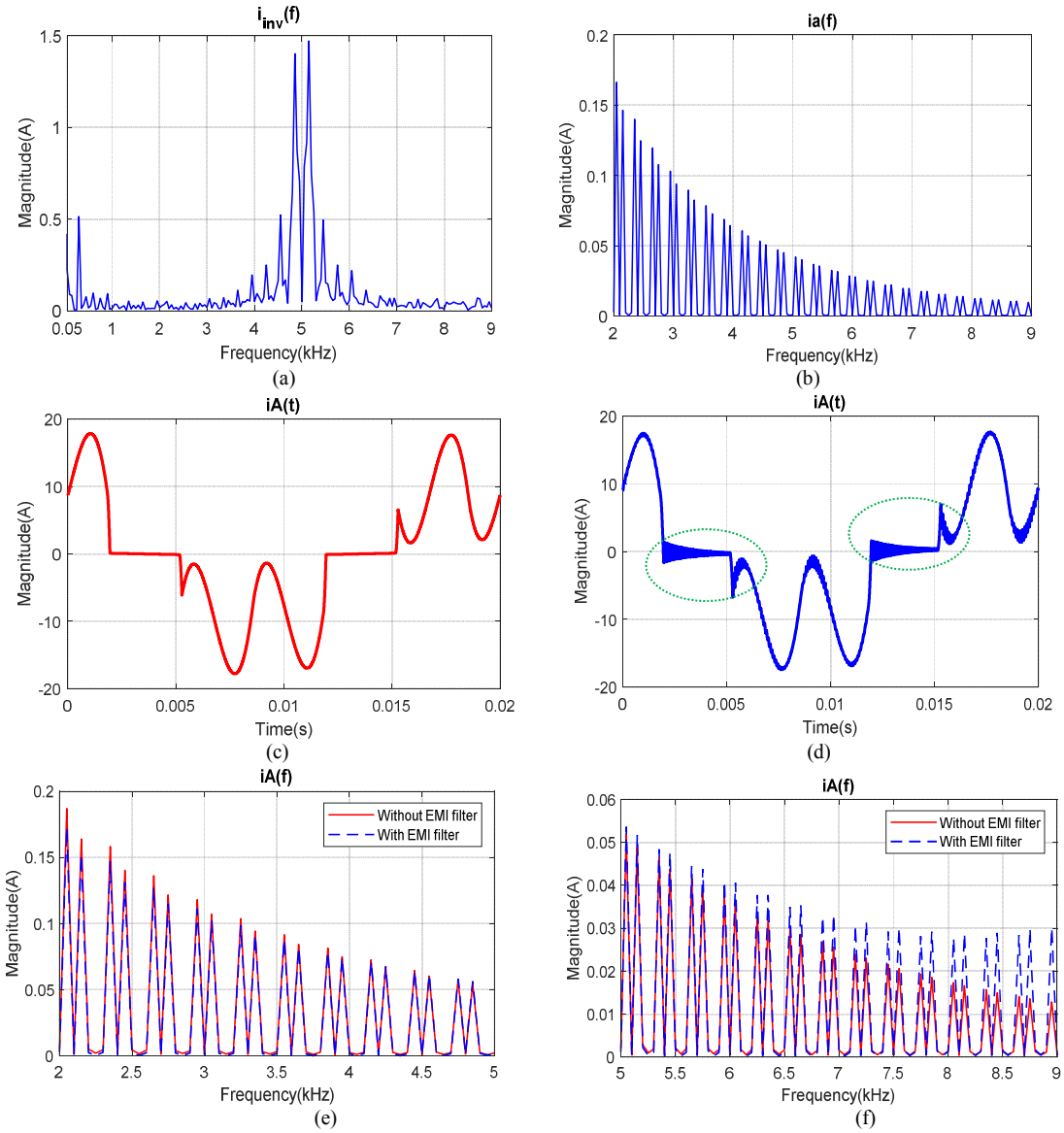

Fig. 2 DM Noise flow in the system (a) frequency spectrum of i_{inv}, (b) frequency spectrum of i_a ,(c) time-domian waveform of i_A-without EMI filter, (d) time-domain waveform of i_A-with EMI filter, frequency spectrum comparison of time-domain waveforms (e) 2-5 kHz, (f) (e) 5-9 kHz

filter, resonance appears at the grid with the non-linearity of the rectifier operation due to the pulse current excitation of the diodes. Apart from that, grid side lossy element and grid inductance have a big impact on the damping of grid current emissions. Hence, even though only two phases conduct through the rectifier, all three phases can be conducted at the grid side through the EMI filter. As the example shown in Fig. 1(b), during each 60º operation of the rectifier, the third phase floats at the rectifier input terminal while creating a circulation path for DM noise at the grid side. Therefore, it is not accurate to model the equivalent circuit assuming a two-phase conduction-mode at the grid side, making the modelling complex. On the other hand, it is not also accurate to model equivalent circuit assuming a three-phase conduction mode at the grid side, since the third phase is always floating from the rest of the system for every 60 degrees. Considering this non-linearity issue of the rectifier, this paper proposes a single-line equivalent circuit model for analysing the DM noise at the grid as depicted in Fig. 1(c) to analyse the transient effects through the EMI filter, assuming the grid side can be represented by three current sources of i_a, i_b and i_c. Multiplication of i_{rect} and switching function of the rectifier, S_a gives i_a as in (3). Even though, [13, 17] have utilized two-phase conduction concept for EMI filter designs, notably this paper only presents the single-line model results based on the above-mentioned facts/concepts, without comparing the existing model in these literatures.

The frequency spectrum of i_A obtained from this single-line model's simulation is compared with that of full model's simulation for a stiff grid (L_g = 0.1 mH, R_g = 0.1 Ω) similar to section II. As shown in Fig. 4(a) simulation results, the error between the three-phase (S3) and single-line modelled i_A (S1) is around 0.1 mA up to 7 kHz and it increases from 7-9 kHz up to -1 mA. The transfer function ($H(f)$) between i_A and i_a are derived for the proposed equivalent model using (4). In this $H(f)$ representation, the grid impedance and impedance across leakage inductor, C_{x1}, and (C_{yAc} together with C_{x2}) are represented as Z_g, Z_{Ldm}, Z_{cx1} and Z_{cycx2}. The derived transfer function over the frequency for the selected grid conditions is shown in Fig. 3, which reveals that EMI filter amplifies the noise coming from the rectifier towards the grid at the frequency range of 2-9 kHz.

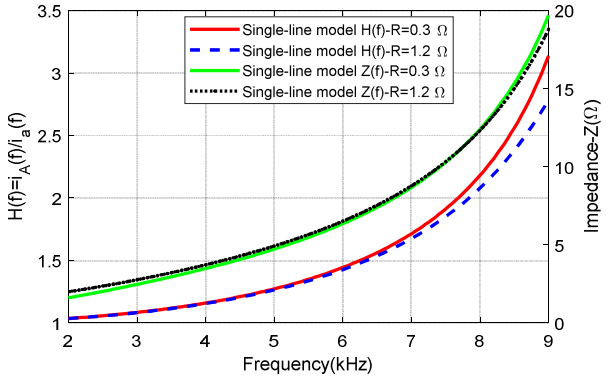

Fig.3 Transfer functions and impedance (Z) of the proposed model

$$H(f)=\frac{Z_{cx1}Z_{cycx2}}{\left(Z_g+Z_{cx1}\right)k-Z_{cx1}{}^2};k=Z_{Ldm}+Z_{cycx2}+Z_{cx1};i_A(f)=H(f)i_a(f) \quad (4)$$

The mathematically calculated $i_A(f)$ using this derived transfer function and the same $i_a(f)$ in Fig. 2(b), is also depicted in Fig. 4 (b). According to the error results in Fig. 4(a) and Fig. 4(b), it is verified both the model-simulation (S1) and model-calculation (C1) give same range of error compared to the frequency spectrum of actual i_A (S3). However, these errors show small deviations of less than 0.2 mA closer to 9 kHz. Thus, either the simulation or calculation approach of the model can be used for DM noise analysis at 2-9 kHz of the three-phase full model, when there is a known i_a (f). The damping of the system is determined by the resistance series with the leakage inductance (R_{dm}) and the grid resistance (R_g). So far, in section II and III, the resultant resistance ($R = R_g + R_{dm} = 0.1\ \Omega + 0.2\ \Omega$) is selected as 0.3 Ω to represent damping factor of a general system. In the following section, the paper presents the effect of this damping factor for the DM noise analysis using the proposed model.

V. Accuracy Evaluation of EMI Filter-Equivalent Model for Different System Damping Conditions

As the system is directly connected to the grid, the noise of i_a at 2-9 kHz highly depends on the grid impedance and the damping factor of the system. As a result, EMI filter response and then the i_A also changes. Considering the damping effect, the paper investigates the accuracy of the single line model of the EMI filter for a highly damped system, where L_g=0.1 mH and R is 1.2 Ω. Here, the R_g is set to 1 Ω, while R_{dm} is kept constant as 0.2 Ω. This condition represents a grid with long distribution lines with high resistance (for example, with low X/R ratio below 0.5). As shown in Fig. 5(a) and Fig. 5(b), the increased damping factor, R has reduced the noise level of i_a and i_A compared to Fig. 2(b) and Fig. 4(a), respectively. As shown, simulation results in Fig. 5(b), the error between the three-phase full model (S3) and modelled i_A (S1) is less than 0.1 mA over the frequency range of 2-9 kHz. Thus, it is clear that the proposed model for DM noise analysis at 2-9 kHz is more accurate for highly damped systems. As shown in Fig. 3, the $H(f)$ also dropped after 7 kHz for the case of a highly damped system. The impedance (Z) plots shown in Fig. 3 verify there is no resonance in the system at 2- 9 kHz, even though Z slightly changes with the selected damping of the system.

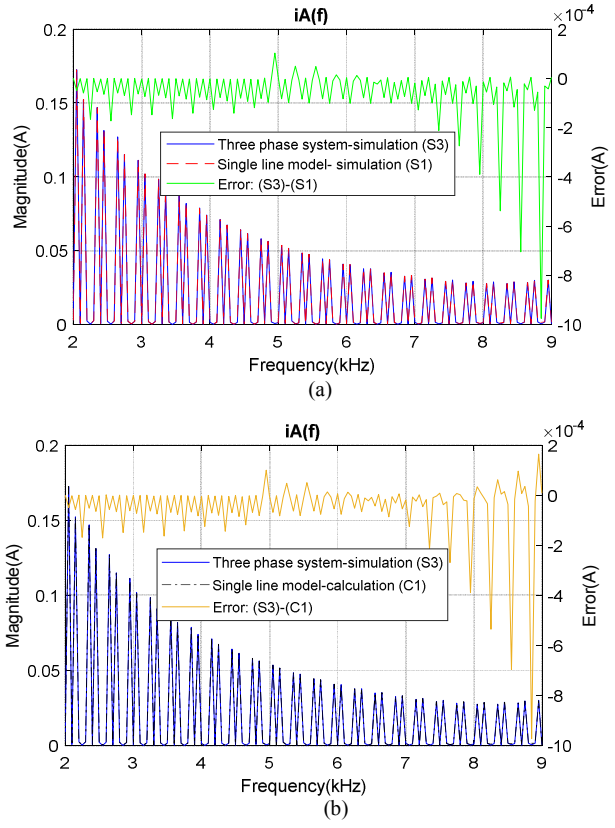

Fig. 4 Accuracy of i_A frequency spectrum using the equivalent circuit of EMI filter (a) single-line equivalent model simulation compared to the three-phase full model simulation, (b) single-line equivalent model calculation using transfer function ($H(f)$) of the model compared to the three-phase full model simulation

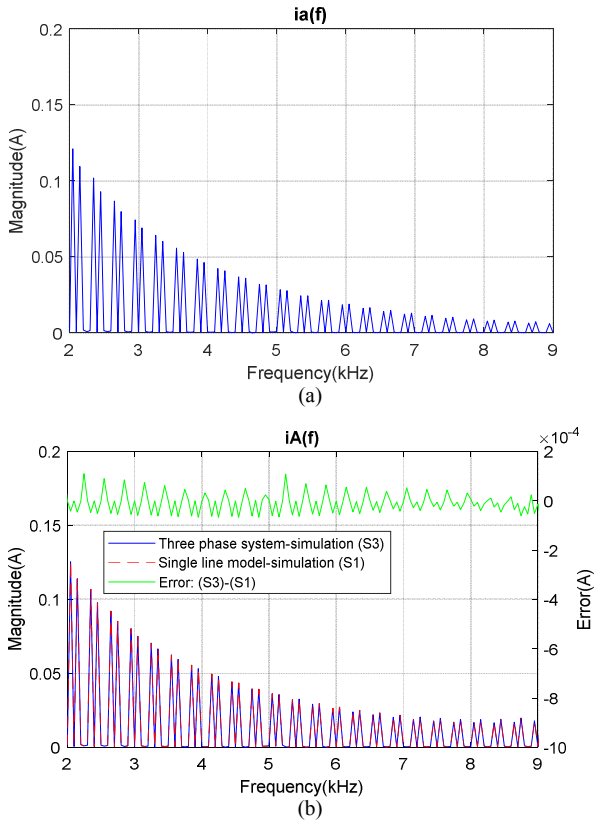

Fig. 5 Accuracy of single-line model of EMI filter under highly damped system condition (R = 1.2 Ω) (a) magnitude of rectifier input current $i_a(f)$, (b) magnitude of grid side current $i_A(f)$

VI. Accuracy Evaluation Of EMI Filter-Equivalent Model For Different Grids

So far, a stiff grid is considered and, in this section, the model accuracy is discussed for a highly damped weak grid, where L_g = 0.1 mH and R_g = 1 Ω. According to Fig. 6(a), the noise level of i_a at 4.5- 5 kHz has increased while there is a noise level drop at the other frequencies compared to that of a stiff grid shown in Fig. 5(a). As shown, simulation results in Fig. 6(b), the noise level of i_A has increased considerably around 3.5 kHz compared to Fig. 5(b). To explain this difference in the weak grid, *H(f)* is compared for the stiff and weak grid. Fig. 6(c) clearly shows that high grid inductance creates a resonance at 3.5 kHz at the grid side with the EMI filter, causing unacceptable noise amplification flowing to the grid. These results of *H(f)* and i_A are comparable in terms of resonance point. As a result, the error between the three-phase full model (S3) and modelled i_A (S1) is also increased at 3.5 kHz as shown in Fig. 6(b). Thus, the accuracy of the model highly degrades, when there is a resonant point created by the high grid inductance of weak grids.

VII. Accuracy Evaluation Of EMI Filter-Equivalent Model For Different Switching Frequencies

In order to further verify the proposed model behaviour at different switching frequencies of the inverter, the system is evaluated with a noise source, i_{inv} consisting of 3 kHz and its multiples of switching noise (See Fig. 7(a)). Even though, there is a change in switching frequency, the frequency response of i_a in Fig. 7(b) is the same as that of 5 kHz switching in Fig. 5(b). It should be noted that the grid is at L_g = 0.1 mH and R_g = 1 Ω, to be able to compare with the results of Fig. 5. As *H(f)* is independent with the switching frequency and i_a is unchanged, the noise level of i_A spectrum is also the same as shown in Fig. 7(c). Moreover, the error between the three-phase full model (S3) and modelled i_A (S1) is less than 0.2 mA, which is acceptable. Thus, it is clear that switching frequency of the inverter load is not an influencing factor, which changes the accuracy of the proposed model for a given system.

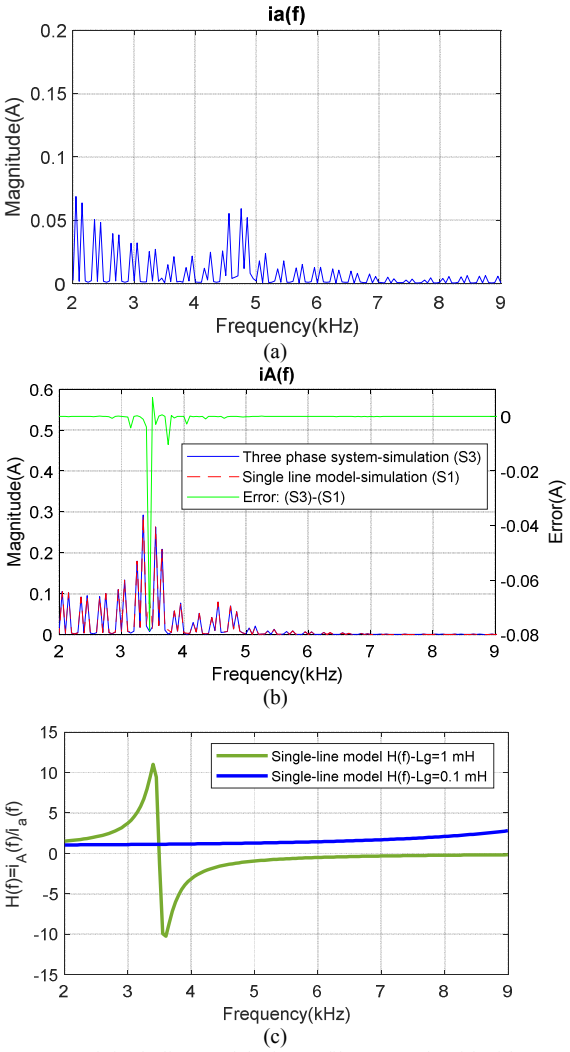

Fig. 6 Accuracy of single-line model of EMI filter at weak grid with L_g = 1 mH (a) magnitude of rectifier input current $i_a(f)$, (b) magnitude of grid side current $i_A(f)$ (c) Transfer function (*H(f)*) of the filter at different L_g

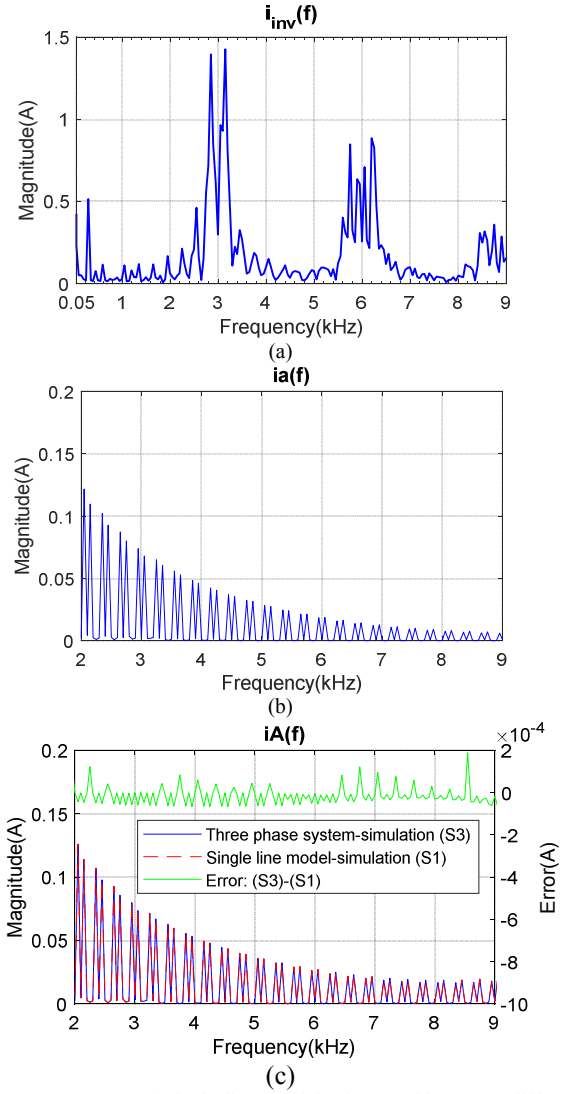

Fig. 7 Accuracy of single-line model of EMI filter at a different switching frequency, 3 kHz (a) frequency spectrum of i_{inv}, (b) magnitude of rectifier input current $i_a(f)$, (c) magnitude of gride side current $i_A(f)$

VIII. Contribution Of Series Resistance Of Leakage Inductor (R_{DM}) For The Noise Reduction At 2-9 kHz

According to the *H(f)* in (4), it is found that R_{dm} in the EMI filter can contribute to reduce the current gain through the filter causing attenuation of the noise of i_A at 2-9 kHz. This can be seen in Fig. 8(c) as well. Further, as discussed, the R_{dm} increases the system damping (R) to reduce the noise of i_a. The simulation results shown in Fig. 8(a) and Fig. 8(b) illustrate

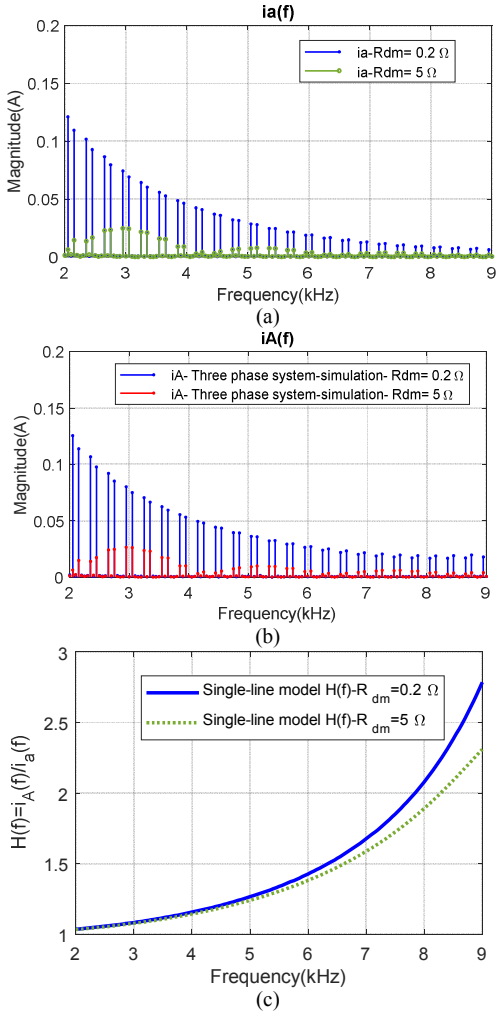

Fig. 8 Emissions with different R_{dm} , 0.2 Ω and 5 Ω (a) frequency spectrums of i_a, (b) frequency spectrums of i_A and (c) *H(f)* of the filter at different R_{dm}

and further verify that high R_{dm} is favourable for noise reduction at 2-9 kHz, both in i_a and i_A. Since, R_{dm} is linked with the system efficiency, there is a limitation in increasing the value of R_{dm} in real application. However, the copper losses of the leakage inductor at high frequency can be increased due to the skin effect improving the damping effect and minimising the losses at low frequency.

IX. Conclusions

This paper presents the possibility of increased grid-side noise level closer to 9 kHz, when there is an input EMI filter connected with a diode rectifier of a three-phase motor drive system, even though there is no resonance introduced by the EMI filter at 2-9 kHz in the case of a stiff grid. The proposed single-line equivalent model of the EMI filter can get rid of transient effects due to the non-linearity of diode rectifier in analysing the DM noise. When the system is with a high damping factor, the accuracy level of the presented model is high for DM noise analysis. If the grid is weak, there can be a resonance with the EMI filter causing unacceptable noise emission to the grid and the model accuracy is low at this resonant frequency. It is found that the model accuracy in predicting grid current is independent of switching frequency of the inverter. Finally, the paper recommends designing optimal series resistance for the leakage inductor considering skin effect at high frequency to attenuate noise at 2-9 kHz.

Acknowledgment

The authors would like to thank the Australian Research Council, supporting FT150100042 and LP170100902 projects.

References

[1] Y. Wang, H. Wen, X. Hou, H. Tang, H. Sun, K. Zheng, S. Li, "Comparison of Differential-Mode and Mixed-Mode Conducted Emission for Household Appliances in Power-Line Communication System," IEEE Trans. on Electromagnetic Compatibility, vol. 59, no. 6, pp. 2023-2028, 2017.

[2] J. Yaghoobi, A. Alduraibi, D. Martin, F. Zare, D. Eghbal, and R. Memisevic, "Impact of high-frequency harmonics (0–9 kHz) generated by grid-connected inverters on distribution transformers," International Journal of Electrical Power & Energy Systems, vol. 122, p. 106177, 2020/11/01/ 2020.

[3] J. Yaghoobi, A. Abdullah, D. Kumar, F. Zare, and H. Soltani, "Power Quality Issues of Distorted and Weak Distribution Networks in Mining Industry: A Review," IEEE Access, vol. 7, pp. 162500-162518, 2019.

[4] D. Darmawardana et al., "Investigation of high frequency emissions (supraharmonics) from small, grid-tied, photovoltaic inverters of different topologies," in IEEE 18th International Conference on Harmonics and Quality of Power (ICHQP), 2018, pp. 1-6.

[5] H. Rathnayake, D. Solatialkaran, F. Zare, and R. Sharma, "Grid-tied Inverters in Renewable Energy Systems: Harmonic Emission in 2 to 9 kHz Frequency Range," in 21st European Conference on Power Electronics and Applications (EPE '19), 2019, pp. P.1-P.10.

[6] H. Rathnayake, K. G. Khajeh, F. Zare, and R. Sharma, "Harmonic Analysis of Grid-tied Active Front End Inverters for the Frequency Range of 0 - 9 kHz in Distribution Networks:Addressing Future Regulations," in IEEE International Conference on Industrial Technology (ICIT), 2019.

[7] K.G. Khajeh, D. Solatialkaran, F. Zare, and M. Nadarajah, "Harmonic Analysis of Grid-connected Inverters Considering External Distortions: Addressing Harmonic emissions up to 9kHz," IET Power Electronics, vol. 13, no. 10, pp. 1934-1945, 2020.

[8] A. Ganjavi, H. Rathnayake, F. Zare, D. Kumar, J. Yaghoobi, P. Davari A. Abbosh, "Common-Mode Current Prediction and Analysis in Motor Drive Systems for the New Frequency Range of 2–150 kHz," IEEE Journal of Emerging and Selected Topics in Power Electronics, pp. 1-1, 2020.

[9] H. Bishnoi, P. Mattavelli, R. Burgos, and D. Boroyevich, "EMI Behavioral Models of DC-Fed Three-Phase Motor Drive Systems," IEEE Trans. on Power Electronics, vol. 29, no. 9, pp. 4633-4645, 2014.

[10] H. Xudong, E. Pepa, L. Jih-Sheng, C. Shaotang, and T. W. Nehl, "Three-phase inverter differential mode EMI modeling and prediction in frequency domain," in 38th IAS Annual Meeting on Conference Record of the Industry Applications Conference, 2003., 2003, vol. 3, pp. 2048-2055 vol.3.

[11] Y. Xiang, X. Pei, W. Zhou, Y. Kang, and H. Wang, "A Fast and Precise Method for Modeling EMI Source in Two-Level Three-Phase Converter," IEEE Trans. on Power Electronics, vol. 34, no. 11, pp. 10650-10664, 2019.

[12] T. Nussbaumer, M. L. Heldwein, and J. W. Kolar, "Differential Mode Input Filter Design for a Three-Phase Buck-Type PWM Rectifier Based on Modeling of the EMC Test Receiver," IEEE Transactions on Industrial Electronics, vol. 53, no. 5, pp. 1649-1661, 2006.

[13] P. Chen and Y. Lai, "Effective EMI Filter Design Method for Three-Phase Inverter Based Upon Software Noise Separation," IEEE Trans. on Power Electronics, vol. 25, no. 11, pp. 2797-2806, 2010.

[14] M. A. Mulla, C. Rajagopalan, and A. Chowdhury, "Compensation of three-phase diode rectifier with capacitive filter working under unbalanced supply conditions using series hybrid active power filter," IET Power Electronics, vol. 7, no. 6, pp. 1566-1577, 2014.

[15] J. Seung-Gi and C. Ju-Yeop, "Line current characteristics of three-phase uncontrolled rectifiers under line voltage unbalance condition," IEEE Trans. on Power Electronics, vol. 17, no. 6, pp. 935-945, 2002.

[16] F. Zare, H. Soltani, D. Kumar, P. Davari, H. A. M. Delpino, and F. Blaabjerg, "Harmonic Emissions of Three-Phase Diode Rectifiers in Distribution Networks," IEEE Access, vol. 5, pp. 2819-2833, 2017.

[17] A. Mallik, W. Ding, and A. Khaligh, "A Comprehensive Design Approach to an EMI Filter for a 6-kW Three-Phase Boost Power Factor Correction Rectifier in Avionics Vehicular Systems," IEEE Trans. on Vehicular Technology, vol. 66, no. 4, pp. 2942-2951, 2017.